

Article

Effects of Germanium Tetrabromide Addition to Zinc Tetraphenyl Porphyrin / Fullerene Bulk Heterojunction Solar Cells

Atsushi Suzuki *, Kenta Nishimura and Takeo Oku

Department of Materials Science, The University of Shiga Prefecture, 2500 Hassaka, Hikone, Shiga 522-8533, Japan; E-Mails: step-by-step623@docomo.ne.jp (K.N.); oku@mat.usp.ac.jp (T.O.)

* Author to whom correspondence should be addressed; E-Mail: suzuki@mat.usp.ac.jp; Tel.: +81-749-28-8369, Fax: +81-749-28-8591.

Received: 15 January 2014; in revised form: 1 February 2014 / Accepted: 24 February 2014 / Published: 4 March 2014

Abstract: The effects of germanium tetrabromide addition to tetraphenyl porphyrin zinc (Zn-TPP)/fullerene (C_{60}) bulk heterojunction solar cells were characterized. The light-induced charge separation and charge transfer were investigated by current density and optical absorption. Addition of germanium tetrabromide inserted into active layer of Zn-TPP/ C_{60} as bulk heterojunction had a positive effect on the photovoltaic and optical properties. The photovoltaic mechanism of the solar cells was discussed by experimental results. The photovoltaic performance was due to light-induced exciton promoted by insert of $GeBr_4$ and charge transfer from HOMO of Zn-TPP to LUMO of C_{60} in the active layer.

Keywords: porphyrin; fullerene; organic solar cell; X-ray diffraction; transmission electron microscopy

1. Introduction

Electronic applications including electronic devices and solar cell systems based on organic semiconductor of fullerenes as electron accepting material at physical-solid-state have been developed [1–11]. For instance, photovoltaic properties of vapor deposited solar cells using bulk heterojunction film of fullerenes/phthalocyanine have been characterized in regard to light-induced

charge separation and photo current behavior [12]. Electronic conductor and optical device of photoactive layer based on porphyrin derivatives have been developed [13–15]. Molecular design and morphological structure of porphyrin is important to control electronic structure with energy levels at highest occupied molecular orbital (HOMO) and lowest unoccupied molecular orbital (LUMO) [16,17]. Donor activity of modified porphyrin in dye-sensitized solar cells is suggested to be one of the key factors in optimizing electronic structure, photovoltaic and optical properties. The effects of the additive in the ternary porphyrin blends on solid-state polymer/fullerene bulk heterojunction solar cells have been focused on improving the photovoltaic performance [18]. The effects of an additive solvent and diiodooctane on the aggregation of a high-efficiency donor polymer and an acceptor molecule of fullerene derivatives have been investigated [19–22]. In addition, the hybrid bulk heterojunction organic solar cells of CdSe-fullerene (C_{60}) composite films with insert of quantum dot have been studied for harvesting light-excited electrons in the active layer [23]. The quantum dot of CdSe, PbSe and PbS nanocrystal has advantage to promote multiple light-induced charge carriers with high energy excitations in a wide range of optical absorption [24–28]. In a previous work, fabrication and characterization of bulk heterojunction of 5,10,15,20-tetraphenyl-21*H*,23*H*-porphyrin zinc (Zn-TPP) and C_{60} has been studied [29]. The light-induced charge separation and charge transfer has been investigated by current density and optical absorption. Copper phthalocyanine/fullerene-based solar cells were also fabricated, and the electronic and optical properties were investigated [30]. Effects of germanium addition to the solar cells were also investigated, which resulted in an increase of power conversion efficiencies of the solar cells. Nanostructures of the solar cells were investigated by transmission electron microscopy and electron diffraction, which indicated formation of germanium compound nanoparticles in the copper phthalocyanine layers. Nanodiamond-based solar cells were fabricated and the photovoltaic properties were investigated [31]. The nanostructures of the solar cells were investigated by transmission electron microscopy and X-ray diffractometry, and the electronic property was discussed.

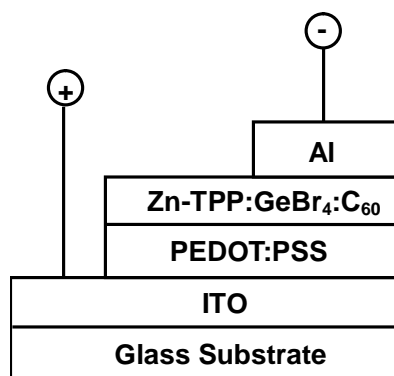
The purpose of this present paper is to investigate additive effect of germanium tetrabromide ($GeBr_4$) on the photovoltaic properties of the Zn-TPP/ C_{60} bulk heterojunction solar cells. The relationship between the photovoltaic properties and microstructure on the bulk heterojunction solar cells with insertion of $GeBr_4$ into the active layers has been focused on optimization of the photovoltaic performance. The photovoltaic mechanism will be discussed by experimental results.

2. Experimental Section

Fullerene (C_{60} , Material Technologies Research, 99.98%), 5,10,15,20-tetraphenyl-21*H*,23*H*-porphyrin zinc (Zn-TPP, Sigma-Aldrich Japan KK, Tokyo, Japan) were used as received. A mixture of C_{60} and Zn-TPP (10 mg) varied with weight ratio with $GeBr_4$ (5×10^{-3} mL, Sigma-Aldrich Japan KK, Tokyo, Japan) dissolved in *o*-dichlorobenzene (1 mL, Sigma-Aldrich Japan KK, Tokyo, Japan) was spin-coated on ITO (A11DU80, AGC Fabritech Co. Ltd., $10 \Omega/\text{sq.}$, Tokyo, Japan). The thickness of the bulk heterojunction films was approximately 150 nm. The heterojunction film was prepared by vapor deposition process using diffusion vacuum pump (10^{-3} Pa, ULVAC Inc., Tokyo, Japan). Heat treatment of these films on the ITO substrate was carried out at 100 °C for 30 min in N_2 atmosphere, aluminum (Al) metal with a thickness of 100 nm was evaporated on a top of electrode. Figure 1 shows

schematic diagram of the present $C_{60}/Zn-TPP$ solar cells as (a) the bulk heterojunction and (b) heterojunction films. Light and dark current density voltage (J-V) characteristics (Hokuto Denko Corp., HSV-100, Kanagawa, Japan) of the solar cells were measured under AM 1.5 (100 mW cm^{-2}) irradiation (Sanei Electric, XES-301S, Tokyo, Japan) in N_2 atmosphere. Optical properties of the bulk heterojunction film of $C_{60}/Zn-TPP$ at solid state were measured by UV-vis spectroscopy (Hitachi U-4100, Tokyo, Japan) and fluorescence photo spectrometer (F-4500 Hitachi, Tokyo, Japan). Internal microstructure was observed by transmission electron microscope (TEM, 200 kV, Hitachi H-8100, Tokyo, Japan) with electron diffraction. TEM is a useful method for nanostructure analysis. The polycrystal structure in the bulk heterojunction film was measured by thin X-ray reflection patterns (X'Pert-MPD system Philips Co. Ltd., Eindhoven, The Netherlands) using $CuK\alpha$ radiation. The chemical structures were optimized by CS Chem3D (Cambridge Soft, PerkinElmer Inc., Boston, MA, USA). Molecular orbital calculations were carried out by MOPAC (Fujitsu Ltd., Tokyo, Japan). In addition, the isolated molecular structures were optimized by quantum calculation using spin-restricted Hartree-Fock method (RHF) using 6-31G* as basis set (Gaussian 03, Gaussian Inc., Pittsburgh, PA, USA). The electronic structures of electron densities with energy levels at HOMO and LUMO were investigated.

Figure 1. Structure of bulk heterojunction solar cells.



3. Results and Discussion

Dark and light induced current density-voltage (J-V) characteristics of the bulk heterojunction solar cells with weight ratio of Zn-TPP and C_{60} with $GeBr_4$ were investigated. The dark J-V curve displayed a gradual increase of current for positive bias to the Zn-TPP electrode. This behavior indicates a light-induced charge separation with charge-transfer at the interface. Table 1 lists measured parameters on the bulk heterojunction solar cell varied with weight ratio of Zn-TPP/ C_{60} to $GeBr_4$.

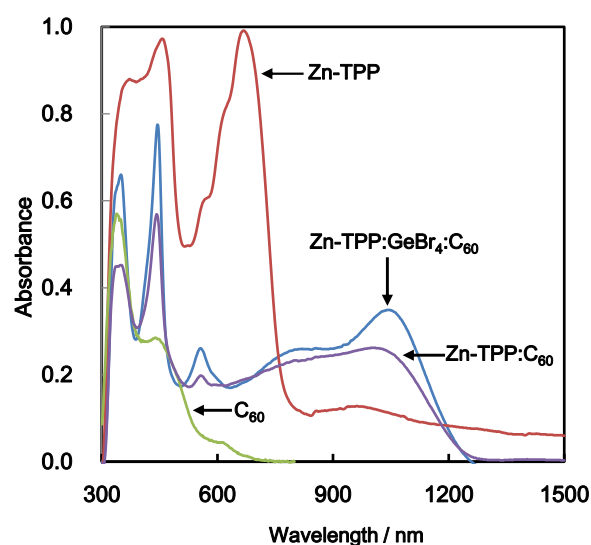
Table 1. Measured parameters on bulk heterojunction solar cells of Zn-TPP/ C_{60} with $GeBr_4$.

Zn-TPP: C_{60}	η (%)	FF	V_{oc} (V)	J_{sc} (mA cm^{-2})
3:7	2.2×10^{-5}	0.23	0.058	0.0017
2:8	9.5×10^{-4}	0.20	0.25	0.019
1:9	1.3×10^{-2}	0.29	0.26	0.17
Additive-free				
1:9	6.4×10^{-3}	0.20	0.23	0.14

At weight ratio of Zn-TPP to C₆₀ of 3:7 by adding GeBr₄, V_{oc}, J_{sc}, FF, and η were obtained to be 0.058 V, 0.0017 mA cm⁻², 0.23 and 2.2 × 10⁻⁵%, respectively. The photovoltaic performance including the measured parameters was gradually improved with increasing weight ratio of C₆₀ in Zn-TPP/C₆₀ by adding GeBr₄. At weight ratio of Zn-TPP/C₆₀ in 1:9, the solar cells performance regarded V_{oc}, J_{sc}, and FF at 0.26 V, 0.17 mA cm⁻² and 0.29, which could estimate to be conversion efficiency of 1.3 × 10⁻²%. As reference case at weight ratio in 1:9 without addition of GeBr₄, the measured parameters, V_{oc}, J_{sc}, FF, and η were obtained to be 0.23 V, 0.14 mA cm⁻², 0.20 and 6.4 × 10⁻³%, respectively. Additionally, quantitative analysis of variable amount of GeBr₄ was performed on the bulk heterojunction solar cell at weight ratio of Zn-TPP/C₆₀ in 1:9. At a fixed amount of GeBr₄ in 0.025 mL, the photovoltaic parameters, V_{oc}, J_{sc}, FF, and η were obtained to be 0.0013 V, 0.0004 mA cm⁻², 0.25 and 1.3 × 10⁻⁷%. The exceed addition reduced the photovoltaic performance. The condition of Zn-TPP/C₆₀ at weight ratio in 1:9 with additive volume of GeBr₄ in 0.005 mL optimized the photovoltaic performance. The photovoltaic properties were due to light-induced charge separation with charge-transfer from HOMO of Zn-TPP to LUMO of C₆₀ in the active layer with insert of GeBr₄.

Optical absorptions of the bulk heterojunction solar cells at weight ratio of Zn-TPP/C₆₀ in 1:9 with insert of GeBr₄ in 0.005 mL are shown in Figure 2. The bulk heterojunction of Zn-TPP/C₆₀ had a strong optical absorption in the range of 300 nm–1300 nm. Especially, insertion of GeBr₄ in the active layer improved the optical absorption in the range of 300 nm–500 nm and 800 nm–1000 nm. The observed absorption at 350 nm, 480 nm to 1050 nm was converted to energy level of 3.5 eV, 2.6 eV and 1.2 eV, respectively. Enlargement of the optical absorption would be attributed from increase of the light-induced exciton in the active layer with insert of GeBr₄.

Figure 2. UV-vis absorptions of bulk heterojunction thin films of tetraphenyl porphyrin zinc (Zn-TPP) and C₆₀ at weight ratio of 1:9 with insert of GeBr₄.



X-ray diffractions of the bulk heterojunction film at weight ratio of Zn-TPP/C₆₀ in 1:9 by adding GeBr₄ on glass substrate are shown in Figure 3. The X-ray diffraction patterns displayed the crystal order of C₆₀, which confirmed tetragonal system noted in crystal index, 111, 220, 311, 220, 420, 422 and 511 in a range of 10° and 33° in 2θ. There existed a strong peak of Zn-TPP with a small peak at

5 ° and 22 ° in 2 θ. The diffraction patterns using the Sherrer’s formula suggested that there were about 6 nm of particle sizes in the tetragonal system. The crystal growth of C₆₀ was inhibited by insertion of the germanium bromide into the active layer. The germanium crystal was not confirmed around 2 θ in the range of 25 °–50 ° [32].

Figure 3. X-ray diffraction patterns of the bulk heterojunction thin films.

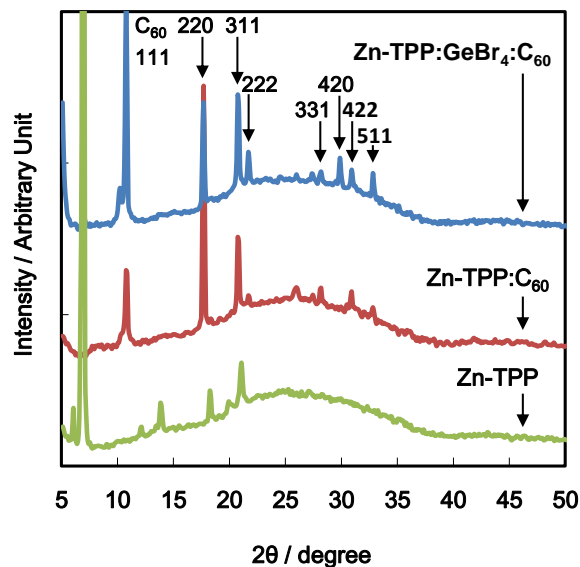


Figure 4. (a) TEM image and (b) electron diffraction pattern of the bulk heterojunction thin film.

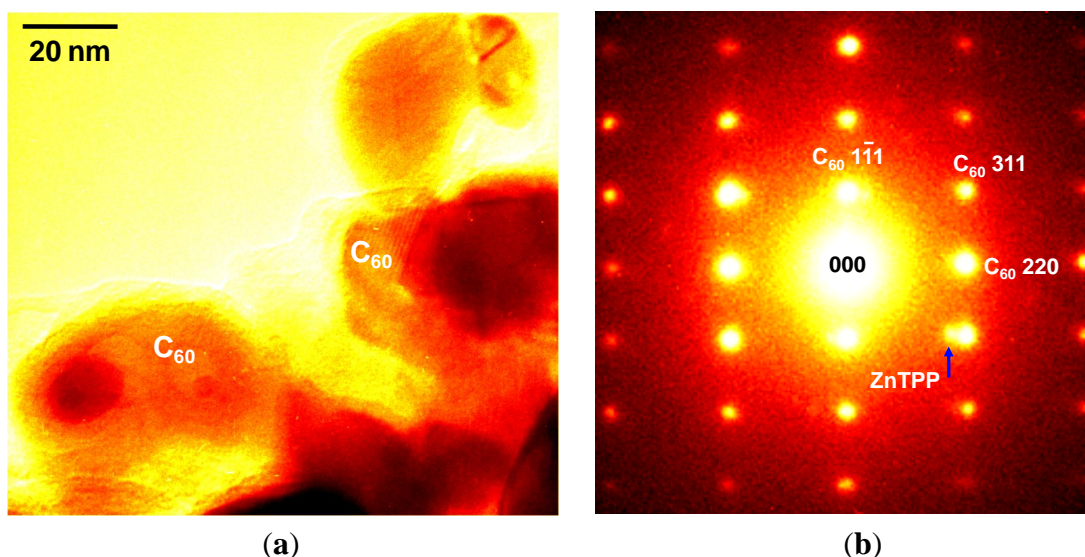


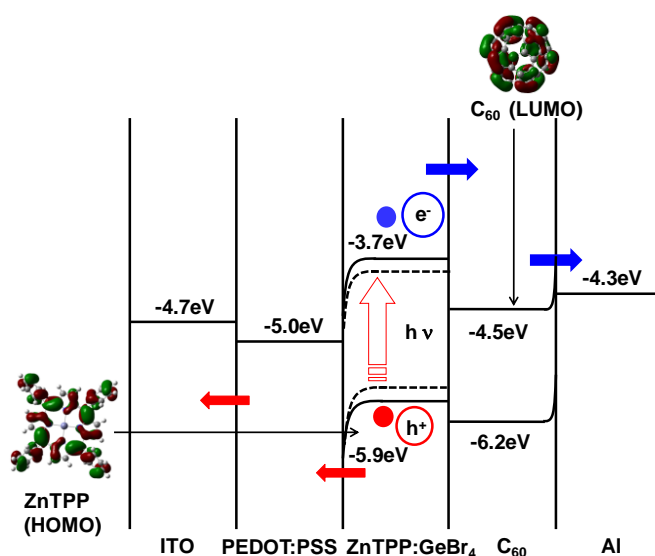
Figure 4 show (a) TEM image and (b) electron diffraction of the bulk heterojunction film at weight ratio of 1:9 with GeBr₄. As shown in Figure 4a, the molecules of C₆₀ were coagulated with each other to form the particle as grain size in the range of 10 nm–20 nm. The TEM image displayed the crystal lattice of C₆₀ to be about 0.38 nm at 111 in crystal index as tetragonal phase in the polycrystal structure. The electron diffraction patterns through the incident angle at $[\bar{1} 1 2]$ indicated that the polycrystal coagulation of C₆₀ had tetragonal structure as noted in crystal index at 111, 210 and 311

with a strong spot as Zn-TPP. The amorphous coagulations were dispersed in the range of 18–30 nm as the particle size. The amorphous coagulations as intrinsic germanium compound appeared to be semi-conductive behavior with a narrow band-gap in the range of 0.8–2.2 eV [33] as shown in Figure 5.

As a reference case to support the experiment result, the coagulations of the germanium compound converted from germanium bromide saturated ionic liquid 1-butyl-3-methylimidazolium hexafluorophosphate on Au (111) has been studied with in-situ scanning tunneling microscopy [34]. The tunneling spectrum of an approximately 500 nm thick germanium compound film saturated ionic liquid on Au (111) suggested semiconductive behavior with a typical band gap of 0.7 eV, which made a good agreement with the value of 0.67 eV for intrinsic coagulations of germanium compound.

In the presence work, insert of coagulations of germanium compound into the active layer improved the light-induced exciton with charge transfer near the interface in microstructure. In actual conditions, energy loss would be generated by the Schottky barrier at the interface between Zn-TPP, C₆₀, and GeBr₄ on Al substrate. The heat treatment of the internal microstructure near interface between the crystal phase of C₆₀ and Zn-TPP with insert of GeBr₄ will guide a considerable support to inhibit recombination between electrons and holes, which will improve the photovoltaic performance with increasing J_{sc} and η in the J-V curve.

Figure 5. Energy level diagram of the bulk heterojunction solar cell.



The photovoltaic mechanism of the bulk heterojunction solar cells was discussed by the experimental results. Schematic energy diagrams of the present solar cells with energy levels were summarized as shown in Figure 5. The photovoltaic mechanism of the present solar cells was discussed as follows. The light irradiation immediately generated charge-separation with a band gap between HOMO of Zn-TPP and LUMO of C₆₀ with insert of GeBr₄. The electrons were excited at a conductive bond, and holes generated at valence band. Suddenly, the excited electrons of Zn-TPP were injected from the conductive band to that of C₆₀ at the crystal phase. In addition, the bulk heterojunction solar cell at an excess amount of C₆₀ showed improvement in the light-induced exciton with an insert of GeBr₄ and the electron diffusion without trapping at interface between inner regions near interface, which suggested an increase of J_{sc} related to carrier mobility, as a result of increasing

the conversion efficiency. In contrast, the holes of Zn-TPP at the valence band suddenly charge-transferred to PEDOT:PSS on electrolyte. V_{oc} of the solar cells were related with an energy gap between HOMO of Zn-TPP and LUMO of C_{60} narrowed with an insert of $GeBr_4$. Controlling the electronic structure and the energy gap between HOMO and LUMO is an important factor for improving the photovoltaic performance with the conversion efficiency. Recently, electronic structures with the energy gap between HOMO and LUMO have been studied by quantum chemical calculation using DFT [16,17].

In this present work, the electronic structures of Zn-TPP with the HOMO-LUMO gap were calculated by DFT. The molecular orbital of Zn-TPP and C_{60} at HOMO, LUMO with the energy levels are shown in Figure 5. Modified porphyrin derivatives combined with phenyl group as electron-donating affinity suggests uniformity on electron density distribution, which becomes a strong donor as p-type semiconductor with a narrow band gap of energy level between HOMO and LUMO. The strong affinity to accept substitutions with a low distribution of electron density in the aromatic ring would support the use of an electron acceptor as n-type semiconductor. The chemical modification of porphyrin has a great advantage to generate light-induced charge separation, suggesting improvement of the photovoltaic performance. Improvement of internal structure would promote injection of electron excitation near interface between Zn-TPP and C_{60} in the internal microstructure. The heat treatment of the microstructure would recover the light-induced charge separation, and then the extent of carrier diffusion, which would result in an improvement of the photovoltaic performance. Additionally, insertion of the semi-conductive coagulations based on germanium compound into the active layer would support the promotion of excitation under the Plasmon field effect.

As an advantage, the coagulations with semi-conductive particles of germanium compound converted from $GeBr_4$ had strong absorption with a low-wave length for improvement of photovoltaic performance. In order to incorporate the coagulations with the semi-conductive particles in the active layer, organic solvent with the coagulations of the particles needs to be used in the manufacturing process. For instance, $GeBr_4$ has melting point at 26.1 °C. The material shows melting characteristics at 30 °C above the melting point and easily dissolves in organic solvent. The material has an advantage when used in dispersion in the organic active layer. By annealing treatment, Ge_3Br_4 was de-composited with removing bromine atom to form the coagulations of the particles under device fabrication condition. The coagulations of amorphous germanium compound into the active layer were dispersed in a range of 20–30 nm in the size. Addition of the coagulations into the active layer had a positive effect on the photovoltaic and optical properties.

Several points of view from cost, toxicity and hazard will be discussed regarding the use of organic solar cells. Additives of $GeBr_4$ have slightly higher cost associated with their industrial application. If mass production using organic layer with $GeBr_4$ is used for applying the organic solar cell, the production cost and price will be reduced in practical use. In the toxicity and hazard points, organic active layer including a large amount of $GeBr_4$ will cause hydrolysis reaction and inflammation on mucosal tissues. However, the experimental condition with a small amount of the coagulations of the particles converted from $GeBr_4$ will be applied for developing safe devices. The organic active layer including the coagulations of the semi-conductive particles had an advantage in improvement of the photovoltaic performance. The photovoltaic mechanism of the solar cells was discussed by experimental results. The photovoltaic performance was originated in the light-induced carrier

separation promoted by insert of GeBr₄ and charge transfer from HOMO of Zn-TPP to LUMO of C₆₀ in the active layer. Instead of inserting the coagulations of the particles, organic solvent with incorporation of silicon compounds and polysilane derivatives will be used for fabrication of an organic solar cell.

4. Conclusions

The effects of germanium tetrabromide addition to Zn-TPP/C₆₀ bulk heterojunction organic solar cells were characterized. The light-induced charge separation with charge transfer was investigated by current density and optical absorption. Addition of GeBr₄ into active layer of Zn-TPP/C₆₀ had a positive effect on the photovoltaic and optical properties. The TEM image, X-ray and electron diffraction patterns showed the crystal lattice of C₆₀ to be about 0.38 nm at 111 in crystal index at the tetragonal phase with a strong spot as crystal structure of Zn-TPP. The coagulations of amorphous germanium compound into the active layer were dispersed in a range of 20–30 nm in size. Addition of the coagulations into the active layer had a positive effect on the photovoltaic and optical properties. The photovoltaic mechanism of the solar cells was discussed by experimental results. The photovoltaic performance was due to the light-induced carrier separation promoted by insert of GeBr₄ and charge transfer from HOMO of Zn-TPP to LUMO of C₆₀ in the active layer.

Conflicts of Interest

The authors declare no conflict of interest.

References

1. Kroto, H.W.; Heath, J.R.; O'Brien, S.C.; Curl, R.F.; Smalley, R.E. C₆₀: Buckminsterfullerene. *Nature* **1985**, *318*, 162–163.
2. Steven, C.E.; Warren, E.P. Theoretical Fermi-Surface Properties and Superconducting Parameters for K₃C₆₀. *Science* **1991**, *254*, 842–845.
3. Allemand, P.-M.; Khemani, K.C.; Koch, A.; Wudl, F.; Holczer, K.; Donovan, S.; Gruner, G.; Thompson, J.D. Organic Molecular Soft Ferromagnetism in a Fullerene C₆₀. *Science* **1991**, *253*, 301–302.
4. Mihailovic, D.; Arcon, D.; Venturini, P.; Blinc, R.; Omerzu, A.; Cevc, P. Orientational and Magnetic Ordering of Buckyballs in TDAE-C₆₀. *Science* **1995**, *268*, 400–402.
5. Lappas, A.; Prassides, K.; Vavekis, K.; Arcon, D.; Blinc, R.; Cevc, P.; Amato, A.; Feyerherm, R.; Gygax, F.N.; Schenck, A. Spontaneous Magnetic Ordering in the Fullerene Charge-Transfer Salt (TDAE)C₆₀. *Science* **1995**, *267*, 1799–1802.
6. Khlyabich, P.P.; Burkhart, B.; Rudenko, A.E.; Barry, C. Optimization and Simplification of Polymer-Fullerene Solar Cells through Polymer and Active Layer Design. *Polymer* **2013**, *54*, 5267–5298.
7. Marrocchi, A.; Lanari, D.; Facchetti, A.; Vaccaro, L. Poly(3-hexylthiophene): Synthetic Methodologies and Properties in Bulk Heterojunction Solar Cells. *Energy Environ. Sci.* **2012**, *5*, 8457–8474.

8. Roncali, J. Single Material Solar Cells: The Next Frontier for Organic Photovoltaics? *Adv. Energy Mater.* **2011**, *1*, 147–160.
9. Brabec, C.J.; Gowrisanker, S.; Halls, J.J.M.; Laird, D.; Jia, S.; Williams, S.P. Polymer-Fullerene Bulk-Heterojunction Solar Cells. *Adv. Mater.* **2010**, *22*, 3839–3856.
10. Liao, H.C.; Tsao, C.S.; Lin, T.H.; Jao, M.H.; Chuang, C.M.; Chang, S.Y.; Huang, Y.C.; Shao, Y.T.; Chen, C.Y.; Su, C.J.; *et al.* Nanoparticle-Tuned Self-Organization of a Bulk Heterojunction Hybrid Solar Cell with Enhanced Performance. *ACS Nano* **2012**, *6*, 1657–1666.
11. Chen, W.; Xu, T.; He, F.; Wang, W.; Wang, C.; Strzalka, J.; Liu, Y.; Wen, J.; Miller, D.J.; Chen, J.; *et al.* Hierarchical Nanomorphologies Promote Exciton Dissociation in Polymer/Fullerene Bulk Heterojunction Solar Cells. *Nano Lett.* **2011**, *11*, 3707–3713.
12. Brousse, B.; Ratier, B.; Moliton, A. Vapor deposited solar cells based on heterojunction or interpenetrating networks of zinc phthalocyanine and C₆₀. *Thin Solid Films* **2004**, *451–452*, 81–85.
13. Donzello, M.P.; Ercolani, C.; Kadish, K.M.; Ricciardi, G.; Rosa, A.; Stuzhin, P.A. Tetrakis (thiadiazole)porphyrazines. 5. Electrochemical and DFT/TDDFT studies of the free-base macrocycle and its Mg^{II}, Zn^{II}, and Cu^{II} complexes. *Inorg. Chem.* **2007**, *46*, 4145–4157.
14. David, C.; Hans, G.; Mathieu, O.; Jef, P.; Paul, H. Stacked organic solar cells based on pentacene and C₆₀. *Solar Energy Mater. Solar Cells* **2007**, *91*, 399–404.
15. Mauro, M.; Matthias, W.; Alberta, B.; Nikos, K.; Sean, S.; Markus, S.; Zhengguo, Z.; David, W.; Russell, G.; Christoph, B. Bipolar Charge Transport in PCPDTBT-PCBM Bulk-Heterojunctions for Photovoltaic Applications. *Adv. Funct. Mater.* **2008**, *18*, 1757–1766.
16. Park, J.K.; Lee, H.R.; Chen, J.; Shinokubo, H.; Osuka, A.; Kim, D. Photoelectrochemical Properties of Doubly β-Functionalized Porphyrin Sensitizers for Dye-Sensitized Nanocrystalline-TiO₂ Solar Cells. *J. Phys. Chem. C* **2008**, *112*, 16691–16699.
17. Ruimin, M.; Ping, G.; Linlin, Y.; Lianshun, G.; Xianxi, Z.; Mohammad, K.N.; Michael, G. Theoretical Screening of –NH₂-, –OH-, –CH₃-, –F-, and –SH-Substituted Porphyrins As Sensitizer Candidates for Dye-Sensitized Solar Cells. *J. Phys. Chem. A* **2010**, *114*, 1973–1979.
18. Dastoor, P.C.; McNeill, C.R.; Frohne, H.; Foster, C.J.; Dean, B.; Fell, C.J.; Belcher, W.J.; Campbell, W.M.; Officer, D.L.; Blake, I.M.; *et al.* Understanding and Improving Solid-State Polymer/C₆₀-Fullerene Bulk-Heterojunction Solar Cells Using Ternary Porphyrin Blends. *J. Phys. Chem. C* **2007**, *111*, 15415–15426.
19. Chen, F.C.; Tseng, H.C.; Ko, C.J. Solvent mixtures for improving device efficiency of polymer photovoltaic devices. *Appl. Phys. Lett.* **2008**, *92*, 103316.
20. Lou, S.J.; Szarko, J.M.; Xu, T.; Yu, L.; Marks, T.J.; Chen, L.X. Effects of Additives on the Morphology of Solution Phase Aggregates Formed by Active Layer Components of High-Efficiency Organic Solar Cells. *J. Am. Chem. Soc.* **2011**, *133*, 20661–20663.
21. Freitas, J.N.D.; Nogueira, A.F. Incorporation of Inorganic Nanoparticles into Bulk Heterojunction Organic Solar Cells. *Nanoenergy* **2013**, doi:10.1007/978-3-642-31736-1_1.
22. Lua, A.J.; Beaupré, S.; Leclerc, M.; Tao, Y. Control of the active layer nanomorphology by using co-additives towards high-performance bulk heterojunction solar cells. *Org. Electron.* **2012**, *13*, 1736–1741.

23. Patrick, B.; Prashant, V.K. Quantum Dot Solar Cells. Electrophoretic Deposition of CdSe-C₆₀ Composite Films and Capture of Photogenerated Electrons with nC₆₀ Cluster Shell. *J. Am. Chem. Soc.* **2008**, *130*, 8890–8891.
24. Nozik, A.J. Quantum dot solar cells. *Physica E* **2002**, *14*, 115–120.
25. Istvan, R.; Vaidyanathan, S.; Masaru, K.; Prashant, V.K. Quantum Dot Solar Cells. Harvesting Light Energy with CdSe Nanocrystals Molecularly Linked to Mesoscopic TiO₂ Films. *J. Am. Chem. Soc.* **2006**, *128*, 2385–2393.
26. Richard, D.S.; Vladimir, M.A.; Victor, C.K. High-efficiency carrier multiplication through direct photogeneration of multi-excitons via virtual single-exciton states. *Nat. Phys.* **2005**, *1*, 189–194.
27. Randy, J.E.; Matthew, C.B.; Justin, C.J.; Pingrong, Y.; Olga, I.M.; Arthur, J.N.; Andrew, S.; Alexander, L.E. Highly efficient multiple exciton generation in colloidal PbSe and PbS quantum dots. *Nano Lett.* **2005**, *5*, 865–871.
28. Luque, A.; Martí A.; López, N.; Antolín, E.; Cánovas, E.; Stanley, C.; Farmer, C.; Caballero, L.J.; Cuadra, L.; Balenzategui, J.L. Experimental analysis of the quasi-Fermi level split in quantum dot intermediate-band solar cells. *Appl. Phys. Lett.* **2005**, *87*, 083505:1–083505:3.
29. Oku, T.; Noma, T.; Suzuki, A.; Kikuchi, K.; Kikuchi, S. Fabrication and characterization of fullerene/porphyrin bulk heterojunction solar cells. *J. Phys. Chem. Solid.* **2010**, *71*, 551–555.
30. Oku, T.; Kumada, K.; Suzuki, A.; Kikuchi, K. Effects of germanium addition to copper phthalocyanine/fullerene-based solar cells. *Cent. Eur. J. Eng.* **2012**, *2*, 248–252.
31. Nagata, A.; Oku, T.; Kikuchi, K.; Suzuki, A.; Yamasaki, Y.; Osawa, E. Fabrication, nanostructures and electronic properties of nanodiamond-based solar cells. *Prog. Nat. Sci.* **2010**, *20*, 38–42.
32. Vijayarangamuthu, K.; Rath, S.; Kabiraj, D.; Avasthi, D.K.; Kulriya, P.K.; Singh, V.N.; Mehta, B.R. Ge nanocrystals embedded in a GeO_x matrix formed by thermally annealing of Ge oxide films. *J. Vac. Sci. Technol. A* **2009**, *27*, 731–733.
33. Ardyanian, M.; Rinnert, H.; Vergnat, M. Structure and photoluminescence properties of evaporated GeO_x/SiO₂ multilayers. *J. App. Phys.* **2006**, *100*, 113106:1–113106:4.
34. Frank, E.; Sherif, Z.E.A. Nanoscale electrodeposition of germanium on Au (111) from an ionic liquid: An *in situ* STM study of phase formation Part I. Ge from GeBr₄. *Phys. Chem. Chem. Phys.* **2002**, *4*, 1640–1648.